Performance of an Electrode Topology for Alkaline Water Electrolysis under Specific Operating Conditions

Maria Jose Lavorante[1,2*], Rodrigo Diaz Bessone[1], Samanta Saiquita[1], Ricardo Martin Aiello[1], Erica Ramirez Martinez[2]

[1]Department of Research and Development, Renewable Energies (CITEDEF-EST), Villa Martelli, Province of Buenos Aires, Argentina

[2]Department of Army Engineering, Defense University, Av. Cabildo, Argentina

*Corresponding author: Maria Jose Lavorante, Department of Research and Development, Renewable Energies (CITEDEF-EST), Villa Martelli, Province of Buenos Aires, Argentina; E-Mail: mlavorante@citedef.gob.ar

Abstract

Channels were machined over the active area of a 316 L stainless steel electrode, in vertical electrode position, with a width of 5 mm that is reduced to 1 mm and then widened again. For its construction, electro discharge machining was selected since it also allows obtaining different degrees of roughness, which can favor the detachment of bubbles to a larger quantity. Analysis of its performance was carried out at an initial operating temperature of 30 ° C and at seven different distances between electrodes, namely: 9.45; 7.45; 6.35; 5.80; 4.30; 2.80 and 2.45 in millimeters, in order to determine the one with the lowest energy consumption to produce a fixed amount of hydrogen. Results obtained from the evaluated distances show that as the distance between electrodes becomes smaller, so do the electrical and transport resistances. The percentage increase in the current density for the distances of 9.45 and 2.45 mm, with respect to the applied potential difference, shows that at 2.2 V it is above 80% (in current density) and is maintained, with small fluctuations throughout the range of applied voltages. Therefore, using the same amount of energy, a greater volume of hydrogen is obtained.

Keywords: *Electrode topology; Alkaline water electrolysis; Distance electrodes*

Introduction

The sustainable supply of energy is presented as one of the main problems of this century. The significant increase in energy, worldwide, is due to the increase in the population added to the increase in living standard [1]. Fossil fuels, on the other hand, will not be able to satisfy the growing demand for energy, due to their inhomogeneous distribution, the fact that the reserves are being depleted and that fewer and fewer oil fields are available for their exploitation. This brings as a consequence, the increase in the price of fuels and governmental ambiguities with the regions that have the largest world reserves. Another problem is directly related to the amount of greenhouse gases that are generated as a result of their burning, which contributes to the climate change. According to the United Nations Conference, which took place at the end of 2015, in Paris, the net emissions of carbon dioxide from the energy sector should be close to zero in 2050, to restrict the increase of the global average temperature below 1.5°C above pre-industrial level [2].

A change of this magnitude would require the generation of energy practically free of carbon dioxide, which would lead the

energy system to rely predominantly on solar and wind energy [3]. The concept of energy conversion Power-to-X, arises as a solution to store energy from intermittent renewable sources as well as to produce carbon-neutral fuels from carbon dioxide emissions [4-5]. Hydrogen production from electricity produced by a renewable resource in energy-to-gas conversion concepts, is promising for future energy storage systems, as hydrogen offers high energy density and can be used without generating emissions [6]. The electrolysis of water, which makes use of the surplus of the renewable resource, is considered a key process for the production of high purity hydrogen. As well as being a well- established technology, used for a long time in various industrial applications, it is expected that, in the near future, it will occupy an increasingly prominent place for decentralized hydrogen production [7]. The electrolysis of water currently must overcome two major challenges, it must minimize energy losses and lowered the cost of the equipment. These points are of vital importance to contribute to the development of the hydrogen economy since the percentage of efficiency of the obtaining process would be raised and production costs would decrease. Although there are many and varied attempts to make the process more efficient, they could be grouped into two large categories: reduce energy consumption and that the energy used is as cheap as possible. Many researchers have focused their work on improving the catalytic activities of the electrodes and thereby reducing the overpotential of the gas evolution reaction.

However, there is another point, in addition to the electrode material, which has a preponderant role above the overpotential that is the effective active area. Effective active area is linked to the roughness of the surface and the latter is pre-established by the preparation/construction of the electrode. This research work presents the results obtained by the use of a triangle shaped topology over 316L stainless steel electrodes, with a certain roughness on the channel surface and seven different distances between electrodes. As the method selected for the construction of the channel, electrical discharge machining, allows achieving different levels of roughness, Charmilles 33 (CH33) was the one selected. Both, the proposed geometry, as well as the method of construction of the geometry over the electrode surface, could be applied to another type of material with a catalytic activity different from the one proposed.

Materials and Methods

Electrode preparation

To evaluate the effect of the roughness generated on the surface of the channel, from the proposed geometry, stainless steel 316 L was selected as the material for the electrodes. Their dimensions are $110 \times 110 \times 3$ millimeters. The electrode surface has two sectors: the rib, where the material is in its original state (as it was acquired from the factory) and the groove (the triangular shaped channel) that has a particular roughness, obtained by the selected method of construction: electrical discharge machining. Figure 1 is an image of the electrode surface.

FIG.1. **The electrode with the triangle shaped topology.**
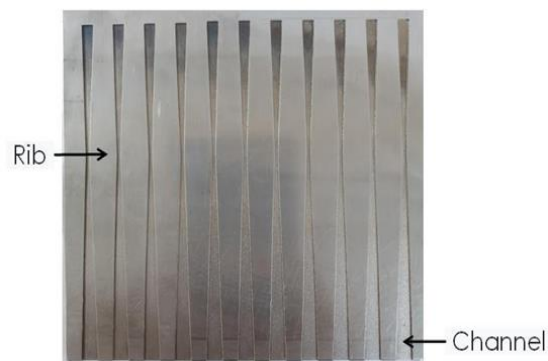
The triangle shaped topology over the electrode surface is obtained by using electrical discharges. This process needs two types of electrodes: The tool and the workpiece. The first one is built of copper with the specific geometry (used in the electroerosion machine) and the other is the object of study, the stainless steel electrode. Recurring current discharges

between these two electrodes, separated by a dielectric liquid and submitted to an electric voltage removed material from the workpiece electrode to generate the desired topology. This is because each spark behaves as a heat source and as a consequence increases the local temperature (>3,000°C) for a very short period of time (from 2 to 100 μs). As a consequence, the material that is heated above the melting temperature is eliminated and carried away by the dielectric fluid [8]. Added to this fact is that the remaining layers of material will undergo changes in their microstructural and mechanical properties [9]. The electro discharge machining is performed on a Charmilles Form 2-Lc machine (Charmilles Technologies), and the dielectric fluid is kerosene.

Since surface roughness is a subject of study in this type of systems, the use of this method allows obtaining different grades because it has a profile-meter. The scale is defined in Charmilles "CH", which is provided to compare commonly used standards such as Ra (Europe)-CLA (UK)-AA (USA). The roughness for the pair of electrodes used in this work is CH33. Charmilles has designated a CH scale, which is, however, cross referenced with the standards that are in common use as roughness average (arithmetic mean deviation, Ra) [10]. Ra is obtained by an algorithm that measures the average length between valleys and peaks and the deviation from the mean line on the entire surface within the sampling length [11]. CH33 equivalent to 4.50 [μm] Ra, exclusively in the channel zone. After the machining process, it is necessary to eliminate the impurities left over the electrode surface applying a cleaning treatment which is composed of the following steps:

- Apply an abrasive cleaner (composed by carbonates, sodium dodecylbenzene and alkalinizing agent among others).
- Wash under tap water.
- Rinse with distilled water, allow to dry.
- Soak some filter paper with acetone (Sintorgan® Pro-Analysis), clean the electrode surface with it and left the electrode to dry.
- Soak some filter paper with ethanol, clean the electrode surface and allow to dry.

In order to analyze the roughness on the electrode surface of the channel, a Scanning Electron Microscope (SEM), Philip SEM 515, is used to produce high resolution images. Micrographs obtained are presented in Results and Discussion section.

Evaluation cell

The evaluation cell consists of: a cubic container; seven pairs of gauges, two guide brackets and two mobile locks. All pieces are constructed in crystal acrylic, except for the stainless steel screws, used to bond and hold some of the mobile pieces. Since it is intended to study the behavior of this specific pair of electrodes at different distances between them, the component of this cell that allow establishing distances is the pair of gauges. There are seven different pairs of gauges, which depending of their size, allow reaching the desired distance. The central piece of the evaluation cell, is the cubic container. Inside it, all the components previously mentioned are placed as well as the electrolyte, the electrodes and the physical separator. Zirfon Perl UTP 500 by Agfa is the material selected as separator. This material is an open mesh polyphenylene sulphide fabric, symmetrically coated with a polymer and zirconium oxide particles [12] which combines good conductivity with a high bubble point and good wettability [13]. The cubic container has in its center and along both walls and base, a channel to fix the separator in a perfectly parallel and equidistant position from the electrodes. A 30% w/w potassium hydroxide (Biopack 85.0%) solution is used as electrolyte.

As a first step, inside the container, the electrolyte is placed, then the separator and finally, at both sides of the separator the pairs of gauges. Before proceeding with the assembly of the cell, it is necessary to mount the electrodes with the guide brackets through the use of stainless-steel screws. The guide brackets have a notch that allows them to rest on the gauges and act as support for the electrodes and, allowing the electrodes to be parallel and equidistant between them and with respect to separator. One the electrode-guide bracket set is assembled, the guide bracket is positioned over the corresponding gauge. The function of the mobile blocks is to secure the position of the guide brackets and the gauges along the determination, and most importantly, the distance between electrodes.

Once the electrode evaluation cell is assembled the electrodes are connected directly to the power supply TDK-Lambda 12,5 V /60 A, by copper wires. After this operation, the real distance between electrodes is determined. It must be taken into consideration that the distance between electrodes obtained, is the result of the size of the gauges and the thickness of the plates used as electrodes. To know more details about the electrode evaluation cell, it is possible to consult the manuscripts.

The analysis of each distance proposed is performed at least four times, if no unexpected variation of the results is found. In case this happens, the determination would be executed 4 extra times, for the detection of the possible cause and discard the wrong determinations for the correct analysis of the results. The analysis includes the calculation of the standard deviation and the corresponding relative error. Table 1 shows the operating parameters studied for the surface finish, CH33.

TABLE 1. **Operating conditions studied: Space between electrodes and temperatures.**

Electrodes	Temperature (ºC)	Space between electrodes (mm)						
CH33 4.5 (μm) Ra	30	9.45	7.45	6.35	5.8	4.3	2.8	2.45

The initial working temperature of 30 ºC is fixed, in order to compare the results and the determinations so, before starting a series, the system is brought to the defined working temperature, setting the system into operation. Once the temperature is reached, the experiment is initiated. The potential difference varies from 0.1 [V] every 30 seconds along a voltage applied difference from 0 to 3.

Results and Discussion

Evaluation of the surface area

The electro discharge machining leads to surface changes that depend specially on the electric energy converted into heat on the surface of the electrode and on the machining conditions. As it was mentioned previously, the electrodes have two well-defined areas: the ribs and the channels. The surface morphology in the channel zone of the electrode is presented below (Figure 2). At this point it is important to highlight, that the incorporation of the channels in the form of opposing triangles increases the area of the electrode by approximately 16% and that the surface generated from the machining method has not been incorporated in that value.

FIG.2. **SEM micrographs of surface channel zones in CH33 electrode: a) rougher 100 x and b) smoother 100 x.**
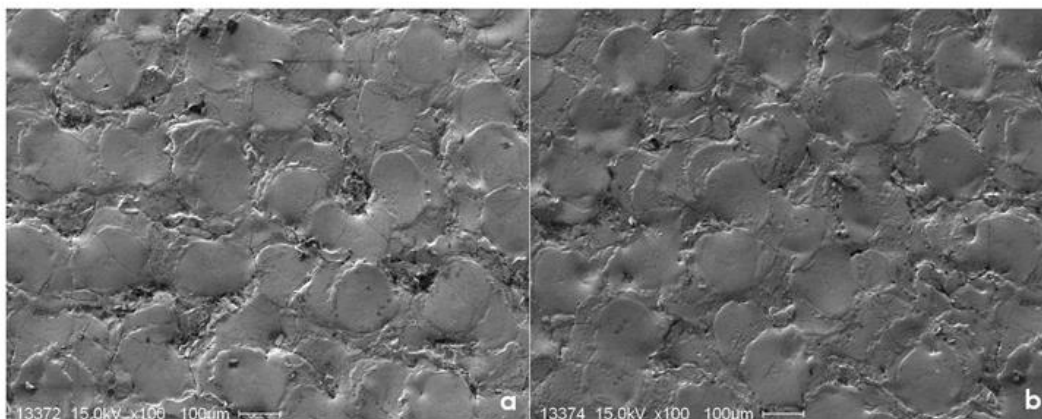
Although both zones seem to have the same types of surface defects (cracks, globules, etc.) The micrograph of Figure 2a presents more marked thermal cracks, deposition of resolidified material than the one in Figure 2b. The reduction in cracks distribution on surface defects could be the result of a modification in the discharge energy and the decrease of the spark intensity along the machining process.

Distance between electrodes

Below are the polarization curves that arise as a result of evaluating the pair of electrodes at different distances between them (FIG. 3). Authors want to clarify that since the distances are obtained by rectified acrylic blocks (gauges), it is difficult to follow a pattern, only the one that arises from the combination of the size of the blocks and the thickness of the electrodes. Data was divided in two groups to facilitate the understanding of the information. The first one comprising values between 10 and 5 millimeters, the second one, values smaller than 5 millimeters.

FIG.3. **Polarization curves per unit area for the analyzed distances between electrodes: (a) 9.45; 7.45; 6.35 and 5.80, and (b) 4.30; 2.80 and 2.45 millimeters.**
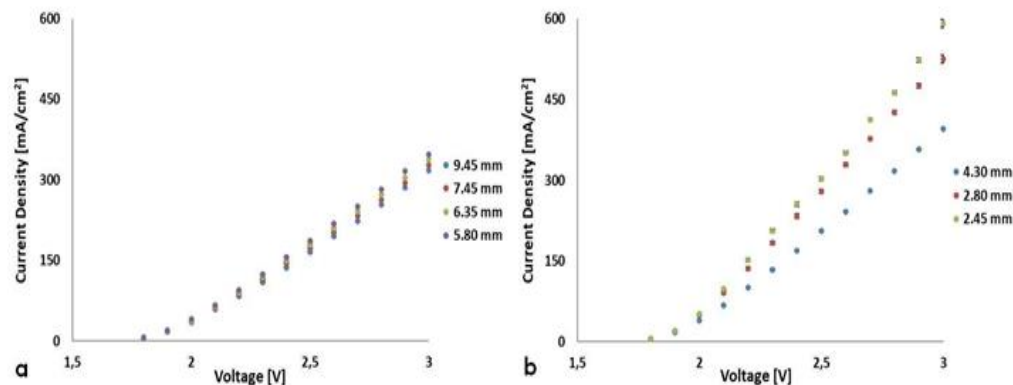
The polarization curves show that for the seven distances evaluated the smallest are those with the highest current densities (2.80 and 2.45 mm). A first fact to highlight in the behavior of the system is that in the results obtained with the distances between 9.45 to 5.80 mm, the increase in current density is gradual (see Figure 3.a.). For the experiments where distances between electrodes are smaller, (from 4.30 to 2.45 mm) the increase in current density is more noticeable (see Figure 3.b.). The standard error for each point, which makes up the polarization curves, is plotted. Unfortunately, as the values are so small, it cannot be appreciated.

The obtained average standard deviation is about 1.23 within the determinations from 10 to 5 mm and 3.86 since 5 mm. The average standard errors are approximately 0.60 and 1.93, respectively. Given that the system with the best performance is the one with a distance between electrodes of 2.45 mm, a graphical representation is constructed showing the percentage of increase in current density that presents the smallest distance evaluated with respect to the others. As can be seen in Figure 4, the most remarkable improvements appear in greater distances that separate both electrodes. To give an example, at an applied voltage difference of 2.3 V, it reaches a value of approximately 89%. It is up to the distance between electrodes of 4.30 mm, where the improvements of current density reach 54%. From that distance, the enhancements are not so significant.

Figure 5, represents the current density and its increment at 2.3 V for all the distances analyzed. Here it can be seen in more detail that, up to a distance of 4.30 mm, between electrodes, the increase in current density is proportional and after that value, there is a change in the slope of the straight line. Something similar occurs with the increase of current density, where an abrupt change in the behavior is also obtained at the same distance.

FIG. 4. **Percentage of increase in current density with respect to the closest distance evaluated: 2.45 mm.**
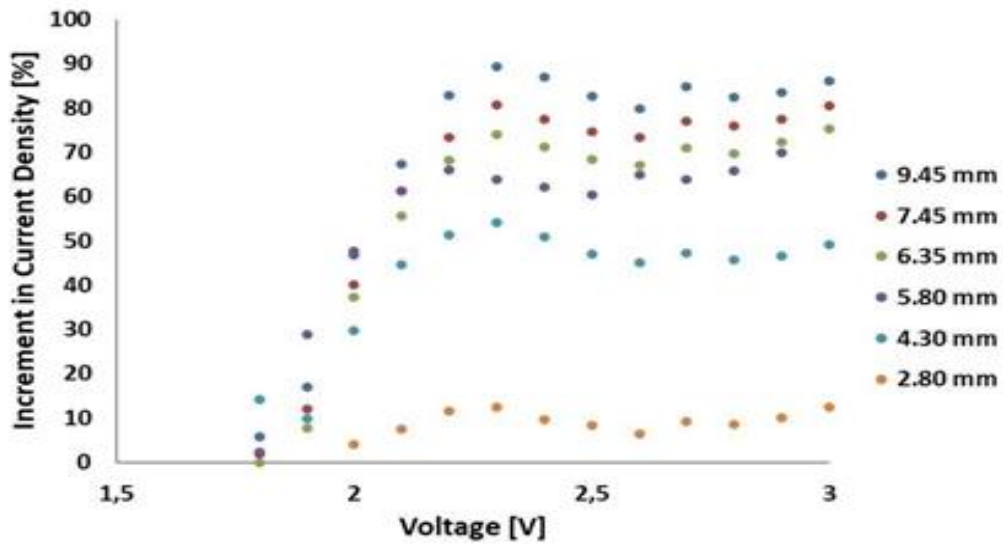
FIG.5. **Current density and percentage of increment for an applied voltage difference of 2.3 V.**
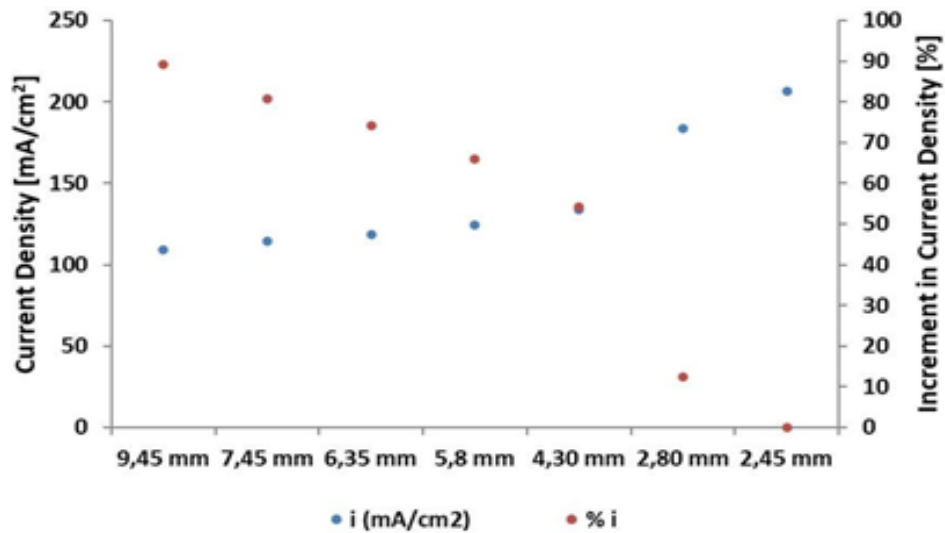
Figure 6 presents the polarization curves of the furthest and closest distances evaluated. At low voltages, close to the water decomposition potential, the differences in current density are not significant, but as the difference in applied voltage is greater, the difference gains importance too. In Figure 6.b., it is observed how at 2.3 V the increment in current density reaches a maximum, close to 89%, which is then partially maintained at higher potentials ($\approx$83%).

FIG.6. a) Polarization curves at 9.45 and 2.45 mm of distances between electrodes and b) percentage of increment in current density between these distances.
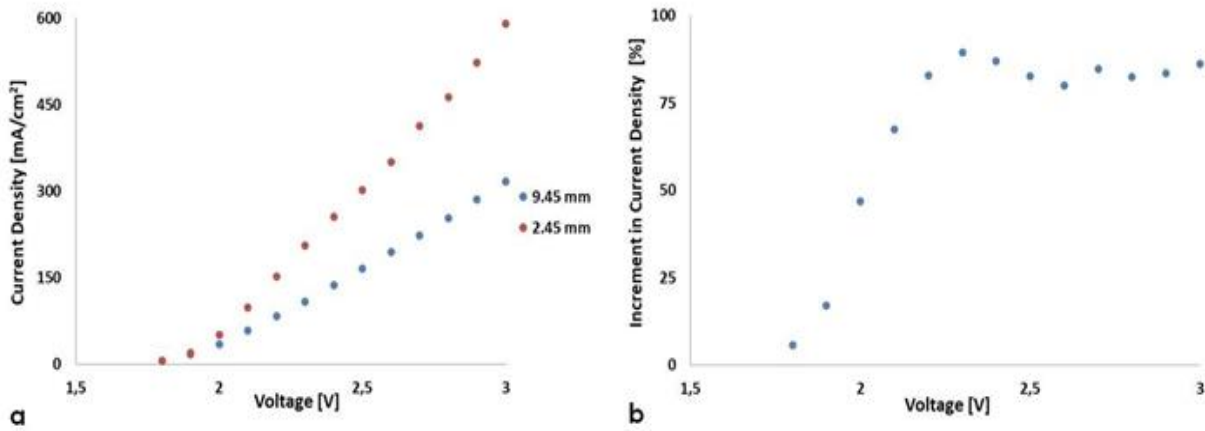
Heat released is the product between the applied voltage difference and the current density. Therefore, the heat released for both systems (9.45 and 2.45 mm) will be discussed. (Figure 7) At the same current density it could be observed that the system where the electrodes are more distant released more heat to generate an equal amount of hydrogen.

FIG.7. Heat released as a function of current density for the 9.45 and 2.45 systems.
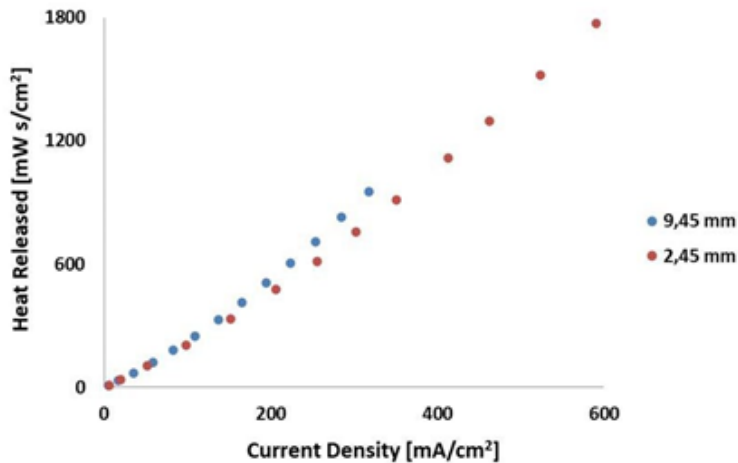
The heat release begins to become perceptible above 100 mA/cm^2. Below that value and as a consequence of the amount of hydrogen generated, there does not seem to be an evolution of any phenomenon that provide loss of energy in the form of heat. The concentration overvoltage and the ohmic loss in the electrolyte become more relevant for the system where the distance between electrodes is bigger. Concentration overvoltage arise from mass transport processes.

Limited mass transport increases the concentration of products between the electrode and the electrolyte and consequently reduces the concentration of reagents. Ohmic losses are the result of the resistance of various cell components, such as current collectors and interconnections just to mention a few, the gas bubbles covering the electrode surface and the material used as diaphragm. To overcome the barriers presented by these phenomena, a higher voltage is required to obtain the same amount of product and the energy losses result in a greater amount of heat released, as can be seen in the graph. As a consequence, higher voltage is required to obtain the same amount of product and the energy losses result in a greater amount of heat released. More research will be conducted to deepen the understanding of these phenomena in this particular system.

Comparison of two electrodes with different roughness surface

Two pairs of electrodes with the same topology were compared in connection with their roughness in order to see if one of them presented better performance than the other. One of the electrodes is the one analyzed previously CH33 with a roughness of 4.50 μm Ra and the other, CH42, has a roughness of 12.6 μm RA. The study of the microstructure of these electrodes by scanning electron microscopy shows that the surface of the electrode with higher roughness presents more defects, like deeper and bigger craters, recast (deposition of resolidified material). As it was previously mention, this could be a consequence of rapid heating and cooling processes.

FIG.8. SEM micrographs of two electrodes with different surface roughness: a) 4.5 μm Ra (100 x); b)12.6 μm Ra (100 x).
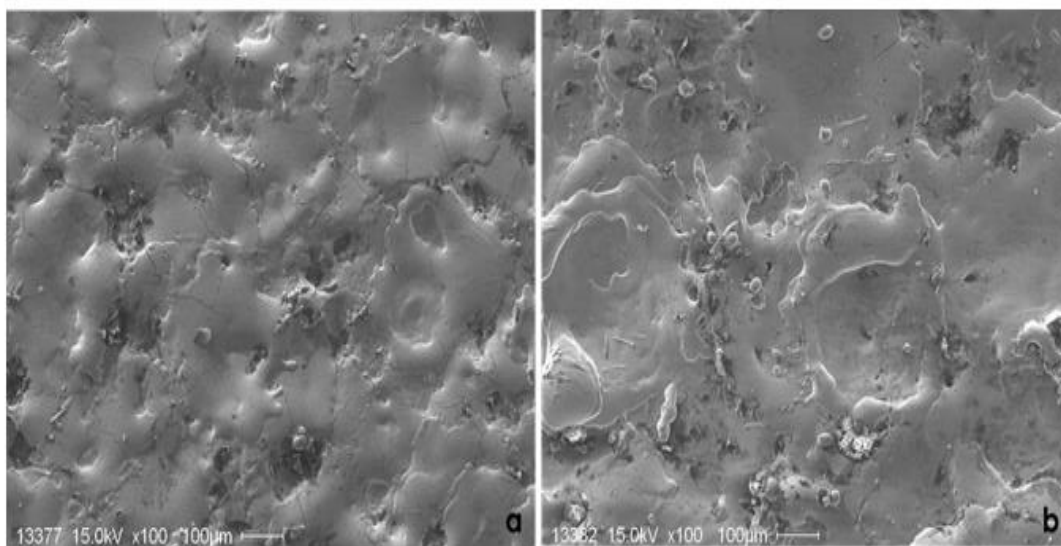
Figure 9 presents the micrographs of an approach of specific zone in both electrodes. It can be observed in more detail that the surface on the electrode with less roughness is smother with few irregularities and thermal cracks along the zone analysed (Figure 9a). On the other hand, the micrograph (Figure 9b.) obtained with the electrode with 12.6 μm roughness presents more irregularities, some of which show deeper craters and more recast material on its surface. Very few thermal cracks are observed in this area and they seem to be more superficial. Subsequently an analysis of the behavior of these pairs of electrodes will be carried out during the electrolysis process.

FIG.9. **SEM micrographs of two electrodes with different surface roughness: a) 4.5 µm Ra (500 x); b)12.6 µm Ra (500 x).**
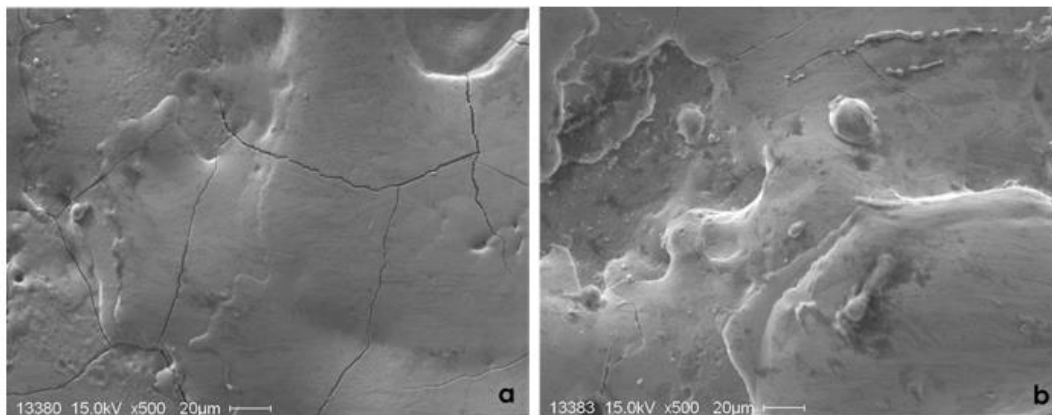
FIG.10. **Polarization curves at different distances between electrodes.**
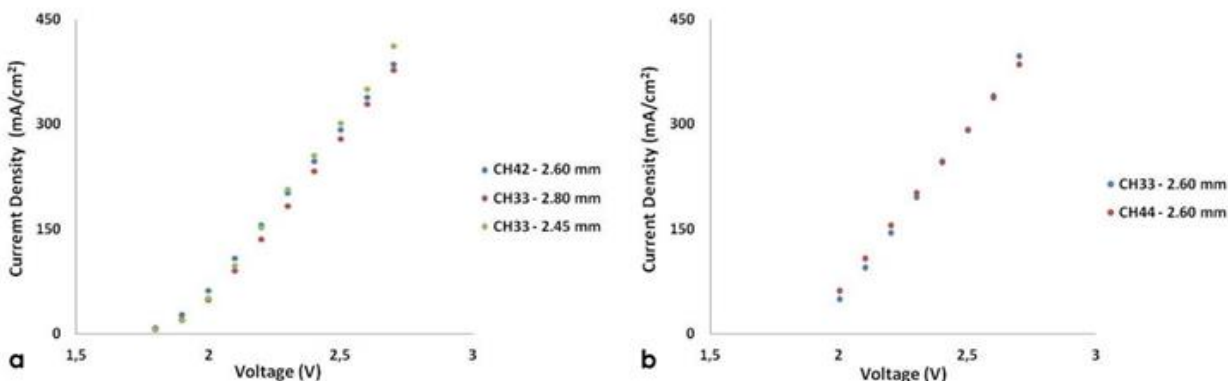
Figure 10a presents the polarization curves of these two pairs of electrodes at different distances between them. Given there are no experiments at the same distance, only those which are similar are represented. This is the reason for representing two determinations of the same pair of electrodes CH33. For the electrode with 4.5 µn Ra (CH33) roughness, the distances between electrodes were 2.8 and 2.45 mm. For the electrode with 12.6 µn Ra (CH42) roughness, the distance represented is 2.60 mm [14]. As it can be seen in the graphical representations, at low applied voltage differences (< 2.3V), the system with the electrodes with higher roughness, presents a better performance than the other. From that potential difference and as the distances between electrodes get shorter, the performance of all the system improves. Figure 10.b represents the extrapolation of the information presented for the electrode with 4.5 roughness at a distance of 2.60 mm, at lower voltage, the current density is bigger in the electrode with higher roughness and at high voltage, the one which performs better is the electrode with lower roughness. This behaviour can be linked to the number of bubbles formed and the way in which those bubbles detach from the surface of the electrodes. The bubbles that are in the vicinity of the electrode are distributed in two areas: The first are those that cover the surface of the electrode while the second are those that rise and disperse in the electrolyte.

From the results it follows that, a more tortuous surface can favor the detachment of the bubbles, when the current densities are less than 200 mA/cm^2. Above this value and with the corresponding increase in quantity, the same tortuosity generates delaying effects on it. Bubbles are absorbed on electrode surface and as a consequence act an electric shield. The bubbles will alter the current distribution and isolate the active sites of the ions involved in the reaction, reducing effective active area.

Conclusion

A pair of electrodes with a roughness of 4.50 μm Ra (CH33) and with a triangle shape topology were analysed. The focus of study was the benefit of reducing the distance between electrodes. The results show that the best performance was achieved at a distance of 2.45 mm at the operating temperature of 30°C. Analysing the heat released by two specific distances shows that the system where the distance was 9.45 mm releases more heat to produce the same amount of hydrogen in comparison with that, with a distance of 2.45 mm. At 2.3 V an increase in current density was of approximately 89%. The result of this work demonstrates that modifying specific configuration conditions, a greater production of hydrogen is obtained making use of the same amount of energy. In connection with the two roughnesses analyzed, a more detailed study should be carried out since the method used to construct the channel is the electro discharge machining. This method promotes significant changes on the surface. The dimension and nature of these changes are determined by the machining conditions and the heat applied on the surface generated by the electric energy. These changes (microstructural, chemical, microgeometrical, surface integrity and mechanical) are the ones that have to be studied in the future for better understanding the behaviour of the systems.

Acknowledgement

References

1. Lehner M, Tichler R, Steinmüller H, et al.. Power-to-gas: Technology and business models. Springer. 2014.

2. Vázquez FV, Koponen J, Ruuskanen V, et al. Power-to-X technology using renewable electricity and carbon dioxide from ambient air: SOLETAIR proof-of-concept and improved process concept. J CO2 Utilizat. 2018;28:235-46.

3. Pleßmann G, Erdmann M, Hlusiak M, et al. Global energy storage demand for a 100% renewable electricity supply. Energy Procedia. 2014;46:22-31.

4. Fuss S, Canadell JG, Peters GP, et al. Betting on negative emissions. Nat Climate Change. 2014;4:850-3.

5. Jangam KV, Joshi AS, Chen YY, et al. Synergistic decomposition of H_2S into H_2 by Ni3S2 over ZrO_2 support via a sulfur looping scheme with CO_2 enabled carrier regeneration. Chem Eng J. 2021;426:131815.

6. Tjarks G, Gibelhaus A, Lanzerath F, et al. Energetically-optimal PEM electrolyzer pressure in power-to-gas plants. Appl Energy. 2018;218:192-8.

7. Sidhom H, Ghanem F, Amadou T, et al. Effect of electro discharge machining (EDM) on the AISI316L SS white layer microstructure and corrosion resistance. Int J Adv Manufac Technol. 2013;65:141-53.

8. Ghanem F, Sidhom H, Braham C, et al. Effect of near-surface residual stress and microstructure modification from machining on the fatigue endurance of a tool steel. J Mater Eng Perform. 2002;11:631-9.

9. Ahn SH, Choi I, Park HY, et al. Effect of morphology of electrodeposited Ni catalysts on the behavior of bubbles generated during the oxygen evolution reaction in alkaline water electrolysis. Chem Commun. 2013;49:9323-5.

10. Ahn SH, Hwang SJ, Yoo SJ, et al. Electrodeposited Ni dendrites with high activity and durability for hydrogen evolution reaction in alkaline water electrolysis. J Mater Chem. 2012;22:15153-9.

11. Vermeiren P, Adriansens W, Moreels JP, et al. Evaluation of the Zirfon® separator for use in alkaline water electrolysis and Ni-H2 batteries. Int J Hydro Energy. 1998;23:321-4.

12. de Groot MT, Vreman AW. Ohmic resistance in zero gap alkaline electrolysis with a Zirfon diaphragm. Electrochimica Acta. 2021;369:137684.

13. Lavorante MJ, Franco JI. Performance of stainless steel 316L electrodes with modified surface to be use in alkaline water electrolyzers. Int J Hydrogen Energy. 2016;41:9731-7.